Nanoscale

PAPER

View Article Online
View Journal | View Issue

Cite this: *Nanoscale*, 2016, **8**, 8118

Smart surface coating of drug nanoparticles with cross-linkable polyethylene glycol for bio-responsive and highly efficient drug delivery†

Weijia Wei,[a] Xiujuan Zhang,*[a] Xianfeng Chen,[b] Mengjiao Zhou,[a] Ruirui Xu[a] and Xiaohong Zhang*[a]

Received 24th December 2015,
Accepted 14th March 2016

DOI: 10.1039/c5nr09167e

www.rsc.org/nanoscale

Many drug molecules can be directly used as nanomedicine without the requirement of any inorganic or organic carriers such as silica and liposome nanostructures. This new type of carrier-free drug nanoparticles (NPs) has great potential in clinical treatment because of its ultra-high drug loading capacity and biodegradability. For practical applications, it is essential for such nanomedicine to possess robust stability and minimal premature release of therapeutic molecules during circulation in the blood stream. To meet this requirement, herein, we develop GSH-responsive and crosslinkable amphiphilic polyethylene glycol (PEG) molecules to modify carrier-free drug NPs. These PEG molecules can be cross-linked on the surface of the NPs to endow them with greater stability and the cross-link is sensitive to intracellular environment for bio-responsive drug release. With this elegant design, our experimental results show that the liberation of DOX from DOX-cross-linked PEG NPs is dramatically slower than that from DOX-non-cross-linked PEG NPs, and the DOX release profile can be controlled by tuning the concentration of the reducing agent to break the cross-link between PEG molecules. More importantly, *in vivo* studies reveal that the DOX-cross-linked PEG NPs exhibit favorable blood circulation half-life (>4 h) and intense accumulation in tumor areas, enabling effective anti-cancer therapy. We expect this work will provide a powerful strategy for stabilizing carrier-free nanomedicines and pave the way to their successful clinical applications in the future.

Introduction

Cancer is a leading cause of death in all countries and chemotherapy has been widely used in combination with other treatments like radiotherapy for curing the disease. However, many current anticancer drugs suffer from serious limitations such as poor water solubility, rapid blood clearance, widespread targeting, low accumulation in disease sites, and detrimental side effects for healthy tissues.[1,2] In an attempt to address these limitations, during the past few decades, many nanovehicles have been developed as drug carriers such as liposomes,[3–5] micelles,[6–9] polymeric nanoparticles (NPs),[10–13] and metal NPs.[14–16] These nanovehicles are able to tremendously enhance the water solubility of drugs and increase their accumulation in tumors *via* an enhanced permeability and retention (EPR) effect,[2] leading to enhanced efficacy and alleviated side effects.[17] Although effective, in these strategies, the carriers do not have a therapeutic function and simply act as a platform to load and transport drug molecules. In this circumstance, these drug carriers are predominantly a major component in the drug system and account for a higher weight portion than actual therapeutics. It apparently leads to a rather low drug loading capacity (DLC). Even worse, many carriers may have potential systemic toxicity when used in the clinic.[18] Recently, pure anticancer therapeutic NPs[19–24] have been developed for a new generation of drug delivery systems, which generally involve the preparation of one or more pure hydrophobic drugs into the form of NPs, and then followed by surface modification with a small amount of surfactants to realize water dispersity and bioenvironmental stability for efficient drug delivery. Such a drug delivery system can substantially boost drug loading capacity and avoid the risk of any unnecessary burden to patients. Nevertheless, this type of drug NPs possess inadequate *in vivo* stability, since the surfactant is anchored to the surface of NPs only through weak hydrophobic interactions. The lack of stability may result in premature drug release following administration into the blood stream.

[a]*Functional Nano & Soft Materials Laboratory (FUNSOM) and Technology Jiangsu Key Laboratory for Carbon-Based Functional Materials & Devices, Soochow University, Suzhou, Jiangsu 215123, China. E-mail: xjzhang@suda.edu.cn, xiaohong_zhang@suda.edu.cn; Tel: +86 512 65880955*
[b]*School of Chemistry and Forensic Sciences, Faculty of Life Sciences, University of Bradford, BD7 1DP, UK*
†Electronic supplementary information (ESI) available. See DOI: 10.1039/c5nr09167e

Herein, in this work, we have synthesized two bio-responsive and crosslinkable amphipathic surfactants which can efficiently minimize any premature drug release from drug NPs during blood circulation and achieve bio-responsive release at the tumor site. Considering that the intracellular concentration of glutathione (GSH) is considerably greater than that in the extracellular environment (~10 mM *vs.* ~2 μM),[25] we developed two types of GSH-responsive molecules including PEG^{5000}-Lys-LA$_2$ (PEG$_A$) and PEG^{5000}-Lys-(Lys-LA$_2$)$_2$ (PEG$_B$). Then they were applied in the surface functionalization of doxorubicin (DOX) NPs for controlled intracellular drug release. The stability, *in vitro* drug release, cytotoxicity, cellular uptake, blood circulation, biodistribution, and anti-tumor activity were systematically studied for different types of NPs including bare DOX NPs, DOX NPs coated with PEG$_A$ and PEG$_B$ (individually termed as DOX-NCLPEG$_A$ NPs and DOX-NCLPEG$_B$ NPs), as well as DOX NPs coated with cross-linked surfactant molecules (termed DOX-CLPEG$_A$ NPs and DOX-CLPEG$_B$ NPs). Compared with other NPs, the cross-linked surfactant modified DOX NPs show much better bio-stability, longer blood circulation time, and promoted drug delivery to tumor sites as a result of the adequately inhibited premature release of payload molecules. This is the first report in which crosslinkable polymer molecules are applied to modify pure drug nanoparticles for improved stability and intracellular environment responsive release. This type of pure drug nanomedicine will have a great potential for clinical applications as it does not contain an extra drug carrier material and is less toxic. We conceive the experimental findings to be of great importance to guide the preparation and application of carrier-free nanomedicines in research and future clinical settings.

Results and discussion

Synthesis and characterization of PEG^{5000}-Lys-(Lys-LA$_2$)$_2$ and PEG^{5000}-Lys-LA$_2$

To exhibit an excellent performance, the amphiphilic ligand molecules should include hydrophilic, hydrophobic and cross-linkable segments. The ratio of hydrophilic segments to hydrophobic and crosslinkable segments is a key factor. Herein, two types of novel ligand, PEG^{5000}-Lys-(Lys-LA$_2$)$_2$ and PEG^{5000}-Lys-LA$_2$, containing hydrophobic and crosslinkable lipoic acid (LA) and hydrophilic PEG were synthesized. The synthetic route of PEG^{5000}-Lys-(Lys-LA$_2$)$_2$ is depicted in Scheme 1. The ^{1}H NMR spectrum of PEG^{5000}-Lys-(Lys-LA$_2$)$_2$ (Fig. 1a) displays signals at 1.85–1.90, 3.51, and 3.69 ppm, attributed to the hydrogen protons in LA, PEG backbone and lysine (Lys), respectively.[26,27] In addition, the molecular weight of PEG^{5000}-Lys-(Lys-LA$_2$)$_2$ in MALDI-TOF Mass Spectrometry (Fig. S4†) was almost identical to the theoretical value comparing it to the starting PEG-NH$_2$.

Preparation and characterization of DOX NPs

DOX NPs were synthesized by a solvent exchange method. As Scheme 2 shows, doxorubicin hydrochloride (DOX·HCl) is firstly converted to being hydrophobic. To achieve this, HCl is removed from the molecule by adding triethylamine (TEA) to DOX·HCl in dimethyl sulfoxide (DMSO) solution in a basic environment. Then the DOX/DMSO solution was injected

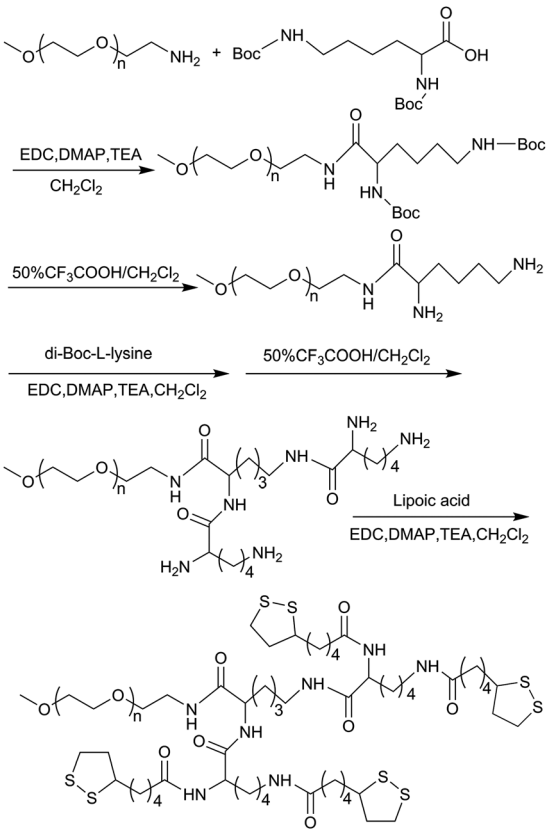

Scheme 1 Synthetic route of PEG^{5000}-Lys-(Lys-LA$_2$)$_2$.

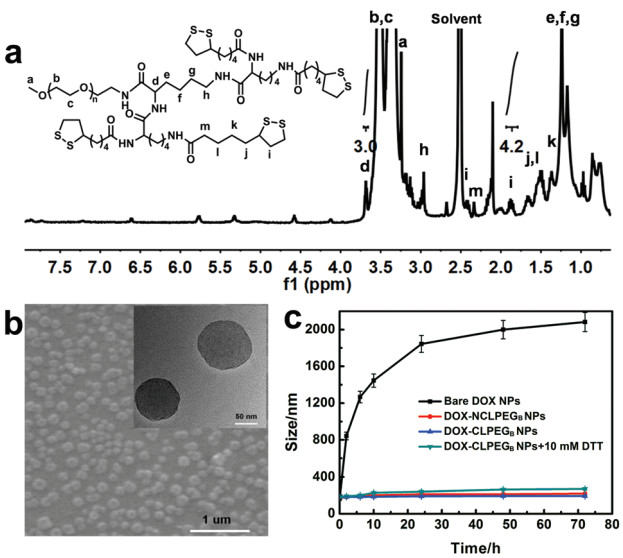

Fig. 1 (a) ^{1}H NMR spectrum of PEG^{5000}-Lys-(Lys-LA$_2$)$_2$. (b) SEM and TEM (inset) images of bare DOX NPs. (c) The evolution of the sizes of different NPs over a period of 3 days.

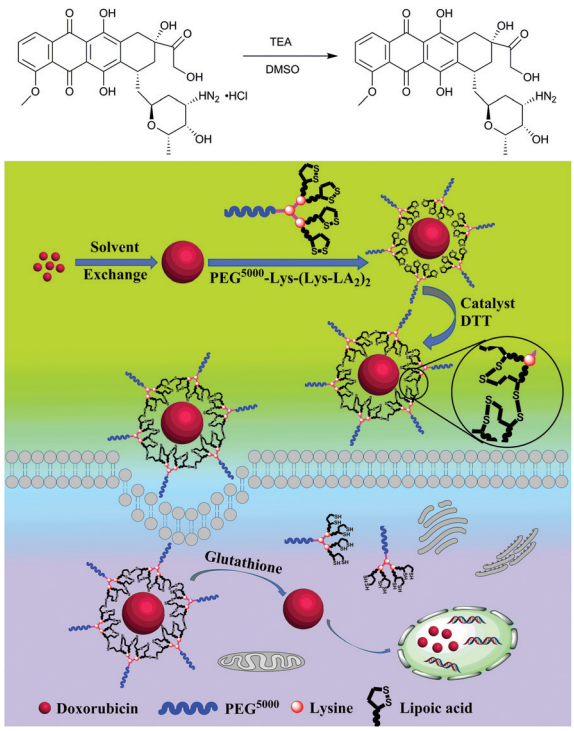

Scheme 2 Schematic illustration of DOX NPs coated by PEG^{5000}-Lys-$(Lys\text{-}LA_2)_2$.

dropwise into water under vigorous stirring to obtain DOX NPs. Subsequently, a solution of PEG_B was injected into the bare DOX NPs suspension to obtain the NPs with non-cross-linked ligands on their surface. To improve the stability of NPs, the surfactant molecules were cross-linked on the surface of NPs by adding dithiothreitol (DTT) to the solution containing DOX NPs and PEG_B under nitrogen. The formation of the cross-link between surfactant molecules can be demonstrated by the apparent change of the absorbance at 330 nm in the UV-Vis absorption spectra of the non-cross-linked PEG^{5000}-Lys-$(Lys\text{-}LA_2)_2$ and cross-linked PEG^{5000}-Lys-$(Lys\text{-}LA_2)_2$ (Fig. S5†).[26]

SEM and TEM images of bare DOX NPs are presented in Fig. 1b. These NPs are mostly spherical and the size is relatively uniform. Dynamic light scattering (DLS) measurement (Fig. S6†) reveals that the average size of these DOX NPs is about 100 nm. After surface modification with PEG_B, the size of the NPs does not change much no matter whether the ligand molecules are cross-linked or not. The stability of these NPs in phosphate buffered saline (PBS) is shown in Fig. 1c. Apparently, PEG_B modified NPs are very stable. During the observation period of 3 days, the size of the surface coated NPs increased only slightly. In great contrast, the bare DOX NPs have poor stability, demonstrated by the dramatic size increase during the same observation time window. Apparently, almost all of the uncoated NPs have aggregated. For the NPs coated with cross-linked PEG_B on the surface, even when we add 10 mM DTT into the solution to break the cross-link, they still remain relatively stable.

Release profiles of DOX from various types of NPs

To understand the influence of the surface modification of DOX NPs on their release profiles, we performed a study by placing various types of NPs in dialysis containers and measuring the release of DOX. In the investigation, we studied three types of DOX NPs including DOX-C18PMH-PEG NPs, DOX-$NCLPEG_B$ NPs and DOX-$CLPEG_B$ NPs. The results are presented in Fig. 2. For the groups of DOX-$NCLPEG_A$ NPs and DOX-$CLPEG_A$ NPs, the results are displayed in Fig. S7.† For DOX-C18PMH-PEG NPs, DOX is rapidly released and about 70% of DOX is released within the first 10 h. For DOX-$NCLPEG_B$ NPs, although the release of DOX is slightly slower, the difference is rather small. Within the same period of the first 10 h, the release only slightly decreases from about 70% to 65%. In a stark contrast, the release of DOX from DOX-$CLPEG_B$ NPs is dramatically alleviated. For the same period of time, only about 15% of DOX has been liberated. Compared to DOX-$CLPEG_B$ NPs, the release of DOX from the DOX-$CLPEG_A$ NPs is slightly higher. About 23% of DOX is released within the same period (Fig. S7b†). The different release profiles between DOX-$CLPEG_A$ NPs and DOX-$CLPEG_B$ NPs may be ascribed to the amount of the LA group in the ligands. PEG_B contains double number of the LA group in

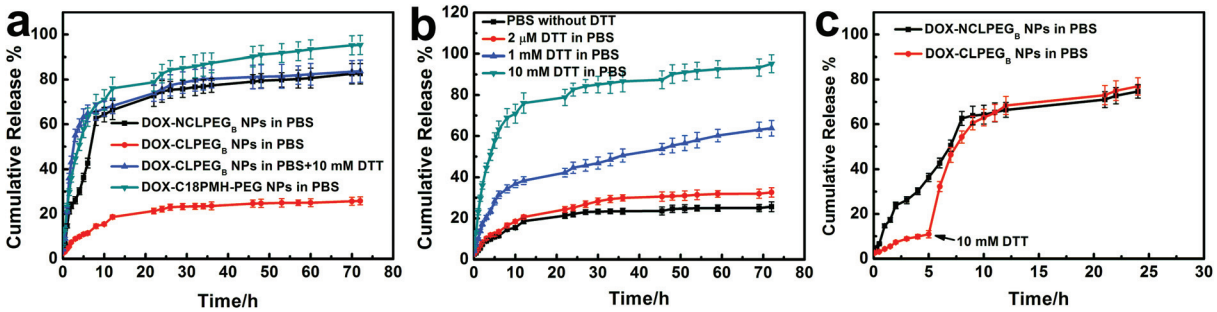

Fig. 2 The release profiles of DOX from different types of NPs and under different conditions. (a) The release profiles of DOX from DOX-C18PMH-PEG NPs, DOX-$NCLPEG_B$ NPs and DOX-$CLPEG_B$ NPs. (b) The release profiles of DOX-$CLPEG_B$ NPs in the presence of different concentrations of DTT in PBS. (c) The release profiles of DOX-$NCLPEG_B$ NPs and DOX-$CLPEG_B$ NPs. For the DOX-$CLPEG_B$ NPs, the release was in PBS for the first 5 h. After 5 h, 10 mM DTT was added to the solution.

comparison with PEG_A, which leads to double cross-linked disulfide bonds in the DOX-$CLPEG_B$ NPs.

To demonstrate that the improved retention of DOX within the DOX-$CLPEG_B$ and DOX-$CLPEG_A$ NPs is due to the cross-linked ligand molecules, we purposely added 10 mM DTT into the solution to break the cross-linking. This amount of DTT is similar to the level of intracellular GSH. Expectedly, the release of DOX from the NPs sharply increases and the profile is almost the same as that of the NPs without cross-linked PEG molecules on the surface (Fig. 2a). In consideration of the release profile of DOX from NPs, PEG_B seems a very suitable surfactant and can be used to modify nanomedicines for improved blood circulation stability.

When the DTT concentration in dialyzed media is the same as the extracellular level of GSH (2 μM), the release profile from the DOX-$CLPEG_B$ NPs is similar to that in the release media without DTT (Fig. 2b). Notably, the DOX release is gradually promoted as the DTT concentration increases from 2 μM to 1 and 10 mM. This means that the release of drug molecules will only be boosted when the nanomedicine is internalized by cells. This characteristic is very useful in drug delivery.

To further demonstrate that the drug release can be conveniently controlled, we incubated DOX-$NCLPEG_B$ NPs and DOX-$CLPEG_B$ in PBS. For DOX-$CLPEG_B$ NPs, after 5 hours incubation, 10 mM DTT was added to the solution. The results are shown in Fig. 2c. It is obvious that there is a burst of drug release from the NPs with cross-linked PEG^{5000}-Lys-(Lys-LA_2)$_2$ once 10 mM was added. After the burst release of DOX from the NPs with cross-linked surfactant molecules, the subsequent release profiles (after 9 h incubation) of both types of NPs are nearly identical. Overall, as shown in these release profiles, for NPs modified with cross-linked PEG molecules, the premature drug release during circulation can be efficiently inhibited. Also attractively, the release of therapeutic molecules from these NPs is potentially controllable by both intracellular and extracellular environments.

In vitro cellular uptake and cell imaging

The intracellular uptake of DOX-$NCLPEG_B$ NPs and DOX-$CLPEG_B$ NPs was investigated in human cervical cancer (HeLa) cells by using confocal microscopy. Free DOX·HCl molecules were used as a control group. As shown in Fig. 3a, the HeLa cells treated with DOX·HCl for 6 h exhibit more intense fluorescence signals than the two types of NPs. The variation is due to the different internalization mechanisms of free DOX and DOX NPs. Briefly, DOX·HCl molecules enter cells through diffusion and then diffuse further into the nuclei, while NPs are internalized by endocytosis.[28–30] Moreover, we can see that the HeLa cells treated with DOX-$CLPEG_B$ NPs possess stronger fluorescence intensity than those incubated with DOX-$NCLPEG_B$ NPs.[26] The finding is similar for the cells with incubation time of both 6 and 12 h with the NPs. The cellular uptake was also quantitatively studied by flow cytometry analysis and the results are in agreement with the above findings. As shown in Fig. 3f and g, a much greater amount of

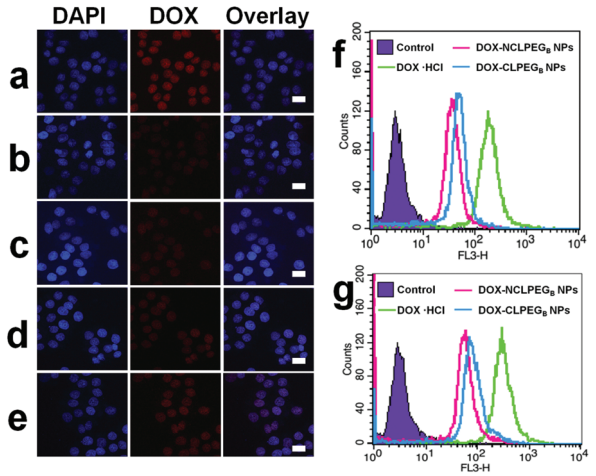

Fig. 3 (a) Intracellular distribution of DOX·HCl in HeLa cells after 6 h incubation. (b, c) Intracellular distribution of DOX-NCLPEGB NPs and DOX-CLPEGB NPs in HeLa cells after 6 h incubation, (d, e) Intracellular distribution of DOX-NCLPEGB NPs and DOX-CLPEGB NPs in HeLa cells after 12 h incubation. Scale bars: 40 μm. (f, g) Flow cytometry analysis of DOX·HCl, DOX-NCLPEGB NPs and DOX-CLPEGB NPs in HeLa cells after 6 h and 12 h incubation.

DOX·HCl is internalized in HeLa cells, when compared with both types of DOX NPs. Additionally, the cells incubated with DOX-$CLPEG_B$ NPs display more intense fluorescence signals than those treated with DOX-$NCLPEG_B$ NPs.

In vitro cytotoxicity of DOX NPs

In vitro cytotoxicity of DOX NPs was assessed with two types of tumor cell lines including mouse metastatic breast cancer cell line (4T1), and HeLa cell line, as well as one type of normal cells, human hepatocytes (HL-7702). In the experiment, DOX·HCl, DOX-$NCLPEG_B$ NPs and DOX-$CLPEG_B$ NPs were cultured with all cell lines at different concentrations ranging from 1.25 to 20 μg mL^{-1} (1.25, 2.5, 5, 10 and 20 μg mL^{-1}) for 24 and 48 h. As presented in Fig. 4a and b, all samples show time and dose dependent cytotoxicity to 4T1 cells. At all concentrations, DOX NPs possess low toxicity than free DOX molecules. For example, after 24 h incubation, at the highest drug concentration of 20 μg mL^{-1}, DOX·HCl exhibits higher cytotoxicity (viability of 23%) than both groups of DOX NPs (viabilities of about 30–40%). This is possibly due to the delayed release of DOX molecules from the NPs inside the cells, while free DOX molecules can easily diffuse through passive diffusion. Meanwhile, as illustrated in Fig. 4c and d, in normal cell line, two types of DOX NPs exhibit dramatically lower cytotoxicity than DOX·HCl. This may be attributed to the high pH and low intracellular GSH concentration in normal cell line in comparison with those in cancer cells.

In vivo blood circulation and biodistribution of DOX NPs

To study whether the cross-link strategy can be applied for inhibiting premature drug release during blood circulation, we intravenously injected DOX-$NCLPEG_B$ NPs and DOX-$CLPEG_B$

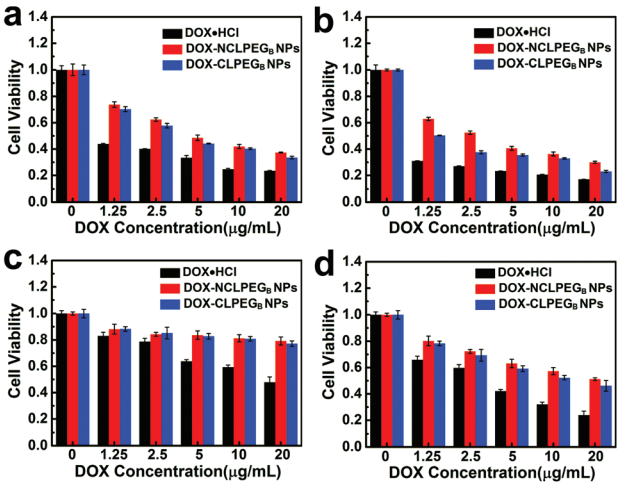

Fig. 4 (a) and (b) Cell viabilities of 4T1 cell lines after being incubated with DOX·HCl, DOX-NCLPEG$_B$ NPs and DOX-CLPEG$_B$ NPs for 24 and 48 h, respectively. (c) and (d) Cell viabilities of HL-7702 cell lines after being incubated with DOX·HCl, DOX-NCLPEG$_B$ NPs and DOX-CLPEG$_B$ NPs for 24 and 48 h, respectively.

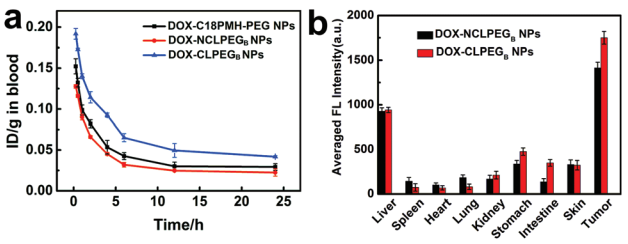

Fig. 5 (a) Blood circulation curve of DOX-C18PMH-PEG NPs, DOX-NCLPEG$_B$ NPs and DOX-CLPEG$_B$ NPs, which was obtained through recording the fluorescence intensities of DOX in the blood at various times after drug administration. The unit is the percentage of the injected dose per gram tissue (% ID g^{-1}). (b) Biodistribution of DOX-NCLPEG$_B$ NPs and DOX-CLPEG$_B$ NPs determined by measuring the fluorescence intensities of DOX in major organs and tumor tissues *in vivo* at 24 h after injection.

NPs into different groups of BALB/c mice. Blood samples were collected at different time points after injection. The mice administered with DOX-C18PMH-PEG NPs were adopted as a control. The fluorescence intensity of each blood sample was recorded and calibrated and the results are presented in Fig. 5a and these indicate that the blood circulation half-life of the DOX-CLPEG$_B$ NPs is much longer (>4 h) than those of the other two types of NPs (~3 h). This indicates that cross-linking surfactant molecules is able to better encapsulate the nanomedicine and enable longer blood circulation time. In other words, the premature release of drug molecules from the nanomedicine can be effectively inhibited.

In vivo biodistribution study was also carried out. Different DOX NPs were intravenously injected into 4T1 tumor bearing mice, and then the fluorescence intensities of DOX in various organs were monitored at different time intervals. Fig. 5b

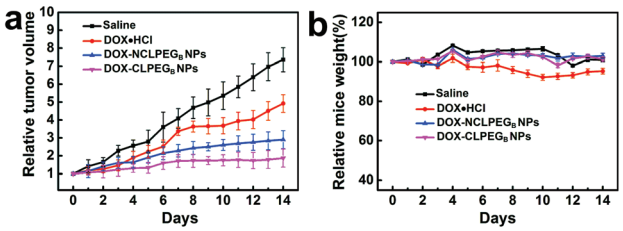

Fig. 6 *In vivo* anticancer effect of free DOX, DOX-NCLPEG$_B$ NPs and DOX-CLPEG$_B$ NPs. (a) The evolution of the tumor volume with time after the mice were administered with saline, free DOX and DOX-NCLPEG$_B$ NPs and DOX-CLPEG$_B$ NPs. Each formulation was injected on Day 0 and 7, and the injection concentration was 1 mg mL^{-1}. (b) Body weight changes with time of 4T1 tumor bearing mice during the treatment period.

shows the biodistribution of DOX in major visceral organs and tumors of the mice treated with the DOX-NCLPEG$_B$ NPs or DOX-CLPEG$_B$ NPs at 24 h post injection. The results clearly demonstrate that the tumors of the mice treated with the DOX-CLPEG$_B$ NPs possess higher levels of DOX. Collectively, all of these outcomes suggest that the cross-link strategy works efficiently and have inhibited premature drug release during circulation. This leads to improved delivery of drug molecules to the tumor sites.

In vivo anticancer activities

To investigate the *in vivo* therapeutic efficacy of the DOX NPs, we chose 4T1 tumor bearing BALB/c mice as an animal model. For tumor treatment, PBS and DOX·HCl, DOX-NCLPEG$_B$ NPs and DOX-CLPEG$_B$ NPs containing 1 mg ml^{-1} of DOX were intravenously administered in different groups of mice. The same treatment was repeated at 7 days after the primary injection. The tumor size and body weight of each mouse were recorded daily for two weeks to quantitatively evaluate the antitumor efficacy. As shown in Fig. 6a, the DOX NPs adequately inhibit the growth of tumor and the therapeutic efficacy is certainly better than the free DOX molecules. Particularly, the DOX-CLPEG$_B$ NPs realize a treatment efficacy (the tumor volume is 1.86 ± 0.41 fold of the initial value), which is clearly better than DOX-NCLPEG$_B$ NPs (2.90 ± 0.49 fold), DOX·HCl (4.92 ± 0.51 fold) and the PBS (7.35 ± 0.66 fold).

Meanwhile, the mice treated with DOX NPs maintain a steady body weight to a certain extent (Fig. 6b). However, the mice which received injection of DOX·HCl experience a drop in body weight probably due to its serious side effect. Apparently, compared with DOX·HCl, the DOX-CLPEG$_B$ NPs can achieve greatly enhanced therapeutic efficiency with alleviated side effects.

Experimental

Materials

DOX·HCl (99%, Beijing ZhongShuo Pharmaceutical Technology Development Co., Ltd), 3-(4,5-dimethyl-2-thiazolyl)-2,5-

diphenyl-2-*H*-tetrazolium bromide (MTT), di-Boc-lysine, DTT and LA (J&K Scientific Ltd) were used as received. Dimethyl sulfoxide-d_6 (DMSO-d_6), 1-ethyl-3-(3-dimethylaminopropyl) carbodiimide hydrochloride (EDC), and 4-dimethylaminopyridine (DMAP) were from J&K Scientific Ltd TEA, DMSO, ethanol, ether, trifluoroacetic acid (TFA) and dichloromethane (DCM) were ordered from Sinopharm Chemical Reagent Co., Ltd. Monomethoxy poly(ethylene glycol) (MePEG-NH_2, MW = 5 kDa, purity >95%) was from Shanghai Yare Biotech, Inc. All reagents and solvents were of analytical grade.

Characterization

^{1}H NMR spectra were obtained from a Unity Inova 400 spectrometer operating at 400 MHz using DMSO-d_6 as a solvent. The chemical shifts were calibrated against residual solvent signals. The mass spectra were collected on a ABI 4700 MALDI-TOF/TOF mass spectrometer (linear mode) using *trans*-2-[3-(4-*tert*-butylphenyl)-2-methyl-2-propenylidene] malononitrile as a matrix. UV-Vis absorption spectra were recorded on a Perkin-Elmer Lambda 750 UV/Vis/NIR Spectrophotometer. The fluorescence spectra were recorded with a FluoroMax 4 (Horiba Jobin Yvon) Spectrofluorometer. Scanning electron microscopic (SEM) images were collected on a FEI Quanta 200 FEG field emission scanning electron microscope. Transmission electron microscopy (TEM) images were observed using a Tecnai G220. DLS analysis measurements were recorded using a Zetasizer Nano ZS (Malvern Instruments, Malvern, UK).

Cell culture

HeLa cells were cultured in Dulbecco's Modified Eagle's medium (DMEM) and HL-7702 and 4T1 cells were cultured in Roswell Park Memorial Institute (RPMI) 1640 medium. The culture media contain 10% of fetal bovine serum (FBS) and antibiotics including penicillin and streptomycin with 50 units per milliliter at 37 °C under a humidified atmosphere containing 5% CO_2.

Synthesis of PEG^{5000}-Lys-LA_2 and PEG^{5000}-Lys-$(Lys\text{-}LA_2)_2$

Di-Boc-lysine (1.5 eq.) was dissolved in CH_2Cl_2, mixed with EDC·HCl (1.8 eq.), DMAP (1.8 eq.) and TEA (2 eq.) and activated at 37 °C for 4 h. This is followed by mixing with PEG^{5000}-NH_2 (1 eq.), and stirring at room temperature for 24 h. Then the solution was mixed with ice-cold ether. Subsequently, the precipitate was filtered and washed with cold ethanol and ether to obtain purified di-Boc-lysine-PEG^{5000}. The obtained PEG derivative ester was dissolved in CH_2Cl_2/TFA (1 : 1, v/v) and stirred for 2 h at room temperature. Finally, the solvent was discarded and the product was precipitated in cold ether, and washed with cold ethanol and ether.

LA (3 eq.), EDC·HCl (3.6 eq.), DMAP (3.6 eq.) and TEA (4 eq.) were dissolved in CH_2Cl_2 and activated at 37 °C for 4 h, followed by mixing with di-NH_2-lysine-PEG^{5000} (1 eq.). The reaction lasted for 24 h at room temperature under rigorous stirring. The solution was then added into 10-fold volume of cold ethyl ether to precipitate the PEG^{5000}-Lys-LA_2, followed by three washes with cold ethanol and ether.

The NH_2-terminated PEG^{5000}-lysine (1 eq.) was conjugated with di-Boc-lysine (3 eq.) that was pre-activated with EDC·HCl (3.6 eq.), DMAP (3.6 eq.) and TEA (4 eq.) at 37 °C for 4 h. The conjugating reaction was stirred for 24 h at room temperature. After filtration and precipitation, the obtained PEG^{5000}-Lys-(di-Boc-lysine)$_2$ was treated with CH_2Cl_2/TFA (1 : 1, v/v) as described formerly. Then the PEG^{5000}-Lys-$(Lys\text{-}LA_2)_2$ was synthesized with the same procedures as described above by conjugating NH_2-terminated PEG^{5000}-Lys-$(Lys)_2$ (1 eq.) with pre-activated LA (6 eq.).

Preparation and modification of DOX NPs

First, 10 mL of 2 mg mL^{-1} DOX·HCl/DMSO solution was prepared and then 12 μL of TEA (1.5 eq.) was added under a moderate stirring at 25 °C. Through this step, hydrophilic DOX·HCl molecules were converted to being hydrophobic. Subsequently, DOX NPs were synthesized by a dropwise injection of 200 μL of the above prepared hydrophobic DOX in DMSO into 10 mL of water under robust stirring and then the stirring was continued for 5 min. Finally, 400 μL of 1.0 mg mL^{-1} PEG_A and PEG_B aqueous solutions were individually added to two solutions of 10 mL of bare DOX NPs. The mixtures were then ultrasonicated for 5 min followed by 1 h incubation at room temperature to obtain PEG_A and PEG_B modified DOX NPs.

Preparation of DOX-CLPEG NPs

The pH of the above-prepared NPs solution was adjusted to be 8.5 using 0.7 M borate buffer (pH 9.0), and the dispersion was purged with nitrogen for 10 min. The cross-linking of the ligand molecules on the surface of NPs was achieved through the addition of 10 mol% DTT relative to the quantity of the lipoyl units in the surfactant. Subsequently, the solution was stirred under nitrogen for 22 h at room temperature.

Stability of NPs in PBS

The stability study was performed to monitor the evolution of the size distribution of bare DOX NPs, DOX-NCLPEG$_A$ NPs, DOX-NCLPEG$_B$ NPs, DOX-CLPEG$_A$ NPs and DOX-CLPEG$_B$ NPs in PBS.

In vitro release of DOX

The DOX NPs modified by C18PMH-PEG were used as a reference for comparison. The C18PMH-PEG was synthesized as described in our previously published paper.[20] Solutions of 2 mL of DOX-C18PMH-PEG NPs, DOX-NCLPEG$_A$ NPs and DOX-CLPEG$_A$ NPs (2 samples) were injected into separate dialysis cartridges with a 14 kDa MWCO. These cartridges were individually dialyzed against 100 mL PBS at 37 °C except that one cartridge containing DOX-CLPEG$_A$ NPs was dialyzed in 100 mL PBS with 10 mM DTT. At desired time intervals, 1 mL solution was collected from each sample for fluorescence measurement and the dialysis medium was replenished with an equal volume of fresh one. In a separate experiment, cartridges containing DOX-CLPEG$_A$ NPs solution were individually dialyzed against PBS with various DTT concentrations (0, 2 μM and 1 mM) at 37 °C. In another experiment, DTT

(10 mM) was added to the release medium at 5 h after starting dialysis. For the other group of DOX-NCLPEG$_B$ NPs and DOX-CLPEG$_B$ NPs, the experimental design was the same as the above.

The quantity analysis of DOX release was performed through the measurement of its fluorescence intensity by a FluoroMax 4 (Horiba Jobin Yvon) spectrofluorimeter (excitation at 488 nm). The fluorescence spectra of DOX of different solutions were recorded from 520 to 650 nm. The experiments were performed in triplicate and the average was presented for analysis.

In vitro cytotoxicity of NPs

Eighty μL of complete media with HeLa, 4T1, HL-7702 cells were placed into different 96-well plates (~60 000 per well) followed by incubation of 24 h. Next, 20 μL of DOX NPs in PBS of different concentrations were added to each well for incubation (37 °C, 5% CO_2). The concentrations of NPs were 1.25, 2.5, 5, 10 and 20 μg mL^{-1} in different groups. After the addition of DOX NPs, the cells were further incubated for 24 and 48 h, followed by being treated with 20 μL of MTT solution (5 mg mL^{-1} in PBS) for 4.5 h for a standard MTT assay measurement.

In vitro cellular uptake of DOX and DOX NPs

Flow cytometry (FCM) and confocal laser scanning microscopy (CLSM) were performed to study the cellular uptake of the DOX·HCl, DOX-NCLPEG$_B$ NPs and DOX-CLPEG$_B$ NPs. For analysis, HeLa cells were cultured with different DOX materials for 6 h and then washed with PBS three times. Following this, the cells were fixed with 4% formaldehyde for 5 min followed by another 3 times of washing in PBS. The cell nuclei were stained with 4′,6-diamidino-2-phenylindole (DAPI, blue) for 10 min. Then the cells were washed with PBS three times for subsequent confocal fluorescence microscopy imaging using a Leica laser scanning confocal microscope. For FCM, the cells were seeded in 12-well plates (~12 000 cells per well). After incubation, the cells were collected by trypsin and centrifuged at 1000 rpm for 3 min. This process was repeated three times and the cells were washed with fresh PBS. Finally, the cells suspended in DMEM media were analyzed for fluorescence intensity with a flow cytometer (BD Biosciences, USA).

In vivo blood circulation and biodistribution of NPs

All *in vivo* experiments were performed in compliance with the relevant laws and institutional guidelines and also approved by Laboratory Animal Center of Soochow University. Different groups of BALB/c mice were administered with 200 μL of 1 mg mL^{-1} DOX-NCLPEG$_B$ NPs, DOX-CLPEG$_B$ NPs, and DOX-C18PMH-PEG NPs. The circulation of NPs was investigated by measuring the fluorescence intensity of DOX at 560 nm in each blood sample. For the measurement, approximately 10 μL of blood was collected from the tail vein of each mouse at desired time intervals (0.25, 0.5, 1, 2, 4, 6, 12 and 24 h). Each blood sample was dissolved in 1 mL of lysis buffer (1% SDS, 1% Triton X-100, 40 mM Tris acetate). The fluorescence intensities of DOX NPs with a series of concentrations were recorded for a standard calibration curve. This experiment was also run in triplicate and the average results were adopted for analysis.

For the analysis of the biodistribution of NPs, 4T1 tumor bearing mice were injected with solution containing either DOX-NCLPEG$_B$ NPs or DOX-CLPEG$_B$ NPs *via* a tail vein. The dose was 1 mg mL^{-1}. At specific time intervals including 2, 6, 12 and 24 h, the mice were sacrificed. The fluorescence intensities of a number of organs and tissues including liver, spleen, heart, lung, kidney, stomach, intestine, skin and tumors were recorded by the Maestro system. The results were calibrated by subtracting the autofluorescence of individual tissues and organs as well as the background reading using the untreated mouse as a reference group for a semi-quantitative biodistribution analysis.

In vivo antitumor activity

Five to six weeks old female BALB/c mice were raised to developed therapy models for solid tumor by implanting 4T1 cells into the right backside. After 6 days, the volumes of the tumors were estimated to be about 55–90 mm^3. The value was calculated by the equation of volume = $a \times b^2/2$ in which a and b represent the longest and shortest diameters of a tumor. Subsequently, the mice were divided into 4 groups (n = 6) in a random manner. Subsequently, one mg mL^{-1} of DOX·HCl, DOX-NCLPEG$_B$ NPs, DOX-CLPEG$_B$ NPs or PBS solution was administered to the different groups of mice *via* a tail vein injection. The same treatment was repeated at 7 days after the primary injection. The tumor size and body weight of each individual mouse were recorded daily for two weeks.

Conclusion

In summary, we designed and synthesized a GSH-responsive and crosslinkable amphipathic surfactant, PEG-Lys-(Lys-LA$_2$)$_2$, and applied it to modify carrier-free DOX NPs with a cross-linking structure. The release of DOX from NPs with cross-linked PEG-Lys-(Lys-LA$_2$)$_2$ molecules is significantly slower than that from the ones with non-cross-linked ligand coating. This indicates that the problem of premature drug release from carrier-free nanomedicine can be efficaciously solved with surface coating of cross-linked surfactant molecules. In the meantime, for the DOX NPs with cross-linked surface molecules, bio-responsive drug release and efficient intracellular uptake can be achieved. *In vivo* studies show that the DOX NPs coated with cross-linked ligands exhibit favorable blood circulation half-life (>4 h), intense accumulation in the tumor area and potent anticancer efficacy. This work further paves a way of using carrier-free nanomedicines for powerful drug delivery in clinical applications.

Acknowledgements

This work was supported by the National Basic Research Program of China (2013CB933500, 2012CB932400), National

Natural Science Foundation of China (61422403), Natural Science Foundation of Jiangsu Province (BK20131162), QingLan Project, Collaborative Innovation Center of Suzhou Nano Science and a Project funded by the Priority Academic Program Development of Jiangsu Higher Education Institutions (PAPD).

Notes and references

1 R. Haag and F. Kratz, *Angew. Chem., Int. Ed.*, 2006, **45**, 1198–1215.
2 J. Fang, H. Nakamura and H. Maeda, *Adv. Drug Delivery Rev.*, 2011, **63**, 136–151.
3 T. M. Allen and P. R. Cullis, *Adv. Drug Delivery Rev.*, 2013, **65**, 36–48.
4 V. P. Torchilin, *Nat. Rev. Drug Discovery*, 2005, **4**, 145–160.
5 Y. Malam, M. Loizidou and A. M. Seifalian, *Trends Pharmacol. Sci.*, 2009, **30**, 592–599.
6 K. Kataoka, A. Harada and Y. Nagasaki, *Adv. Drug Delivery Rev.*, 2001, **47**, 113–131.
7 D. Le Garrec, M. Ranger and J.-C. Leroux, *Am. J. Drug Delivery*, 2004, **2**, 15–42.
8 Y. P. Li, K. Xiao, W. Zhu, W. B. Deng and K. S. Lama, *Adv. Drug Delivery Rev.*, 2014, **66**, 58–73.
9 F. F. Fu, Y. L. Wu, J. Y. Zhu, S. H. Wen, M. W. Shen and X. Y. Shi, *ACS Appl. Mater. Interfaces*, 2014, **6**, 16416–16425.
10 K. M. Cai, X. He, Z. Y. Song, Q. Yin, Y. F. Zhang, F. M. Uckun, C. Jiang and J. J. Cheng, *J. Am. Chem. Soc.*, 2015, **137**, 3458–3461.
11 H. L. Chu, T. M. Cheng, H. W. Chen, F. H. Chou, Y. C. Chang, H. Y. Lin, S. Y. Liu, Y. C. Liang, M. H. Hsu, D. S. Wu, H. Y. Li, L. P. Ho, P. C. Wu, F. R. Chen, G. S. Chen, D. B. Shieh, C. S. Chang, C. H. Su, Z. M. Yao and C. C. Chang, *ACS Appl. Mater. Interfaces*, 2013, **5**, 7509–7516.
12 J. Q. Jiang, B. Qi, M. Lepage and Y. Zhao, *Macromolecules*, 2007, **40**, 790–792.
13 A. Kumari, S. K. Yadav and S. C. Yadav, *Colloids Surf., B*, 2010, **75**, 1–18.
14 Z. Z. J. Lim, J. E. J. Li, C. T. Ng, L. Y. L. Yung and B. H. Bay, *Acta Pharmacol. Sin.*, 2011, **32**, 983–990.
15 L. Yan, J. F. Zhang, C. S. Lee and X. F. Chen, *Small*, 2014, **10**, 4487–4504.
16 X. Zhou, P. Cao, Y. Zhu, W. G. Lu, N. Gu and C. B. Mao, *Nat. Mater.*, 2015, **14**, 1058–1064.
17 K. J. Cho, X. Wang, S. M. Nie, Z. Chen and D. M. Shin, *Clin. Cancer Res.*, 2008, **14**, 1310–1316.
18 T. M. Allen and P. R. Cullis, *Science*, 2004, **303**, 1818–1822.
19 Y. Li, J. Y. Lin, Y. Huang, Y. X. Li, X. R. Yang, H. J. Wu, S. C. Wu, L. Y. Xie, L. Z. Dai and Z. Q. Hou, *ACS Appl. Mater. Interfaces*, 2015, **7**, 25553–25559.
20 W. Li, Y. L. Yang, C. Wang, Z. Liu, X. J. Zhang, F. F. An, X. J. Diao and X. J. Hao, *Chem. Commun.*, 2012, **48**, 8120–8122.
21 J. F. Zhang, Y. N. Li, F. F. An, X. H. Zhang, X. F. Chen and C. S. Lee, *Nano Lett.*, 2015, **15**, 313–318.
22 J. F. Zhang, Y. C. Liang, X. D. Lin, X. Y. Zhu, L. Yan, S. L. Li, X. Yang, G. Y. Zhu, A. L. Rogach, P. K. N. Yu, P. Shi, L. C. Tu, C. C. Chang, X. H. Zhang, X. F. Chen, W. J. Zhang and C. S. Lee, *ACS Nano*, 2015, **9**, 9741–9756.
23 C. T. Yu, M. J. Zhou, X. J. Zhang, W. J. Wei, X. F. Chen and X. H. Zhang, *Nanoscale*, 2015, **7**, 5683–5690.
24 P. Huang, D. L. Wang, Y. Su, W. Huang, Y. F. Zhou, D. X. Cui, X. Y. Zhu and D. Y. Yan, *J. Am. Chem. Soc.*, 2014, **136**, 11748–11756.
25 S. Mura, J. Nicolas and P. Couvreur, *Nat. Mater.*, 2013, **12**, 991–1003.
26 Y. L. Li, L. Zhu, Z. Z. Liu, R. Cheng, F. H. Meng, J. H. Cui, S. J. Ji and Z. Y. Zhong, *Angew. Chem., Int. Ed.*, 2009, **48**, 9914–9918.
27 P. Y. Sun, H. X. Lu, X. Yao, X. X. Tu, Z. Zheng and X. L. Wang, *J. Mater. Chem.*, 2012, **22**, 10035–10041.
28 H. S. Yoo and T. G. Park, *J. Controlled Release*, 2001, **70**, 63–70.
29 X. W. Dai, Z. L. Yue, M. E. Eccleston, J. Swartling, N. K. H. Slater and C. F. Kaminski, *Nanomedicine*, 2008, **4**, 49–56.
30 Y. Q. Li, Y. L. Tong, R. X. Cao, Z. M. Tian, B. S. Yang and P. Yang, *Int. J. Nanomed.*, 2014, **9**, 1065–1082.